JHEP PROCEEDINGS

International Europhysics Conference on HEP

Measurements of charmed meson lifetimes and the D^0-$\overline{D}^0$ mixing parameter y_{CP} at Belle

Bruce Yabsley*† **on behalf of the Belle Collaboration**

Belle Group, K.E.K., Oho 1-1, Tsukuba-shi, Ibaraki-ken, 305-0801 JAPAN
E-mail: yabsley@bmail.kek.jp

ABSTRACT: We present preliminary measurements of D^0, D^+ and D_s^+ lifetimes, and the D-mixing parameter y_{CP}, based on $23.4\,\mathrm{fb}^{-1}$ of e^+e^- data from Belle.

1. D^0-$\overline{D}^0$ mixing and charm lifetimes

Results on D^0-$\overline{D}^0$ mixing are a valuable tool in the search for "new physics", since D-mixing is suppressed in the Standard Model (SM). The contribution of box diagrams such as figure 1, important in K- and B-mixing, is negligible due to GIM suppression: higher-order processes dominate. The mixing parameters $x \equiv \Delta M/\Gamma_{\rm av}$ and $y \equiv \Delta\Gamma/2\Gamma_{\rm av}$ are expected to have values $x, y \sim \mathcal{O}(10^{-3})$, below the current experimental sensitivity [1].

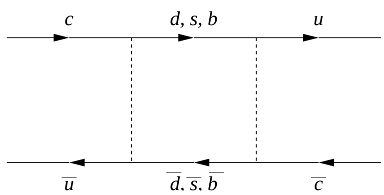

Figure 1: A box diagram for D-mixing in the Standard Model.

In many models of physics beyond the SM, exotic particles participate in new box diagrams and contribute to x (but not y), so the observation of $x \gg y \sim \mathcal{O}(10^{-3})$ has long been considered a signal of new physics. Searches for "wrong-sign" (WS) semileptonic D^0 decays [2], a mixing contribution to WS hadronic decays [3], and lifetime differences between D^0 decay modes [4, 5, 6], have been performed. The FOCUS measurement [5] of

$$y_{\rm CP} \equiv \frac{\Gamma(\text{CP even}) - \Gamma(\text{CP odd})}{\Gamma(\text{CP even}) + \Gamma(\text{CP odd})} \approx \frac{\Gamma(D^0 \to K^- K^+)}{\Gamma(D^0 \to K^- \pi^+)} - 1,$$

$(3.42 \pm 1.39 \pm 0.74)\%$,has created interest due to its size and apparent tension with CLEO [3], although comparison of different types of measurement is difficult (figure 2).

Here, we present preliminary results from Belle on D^0, D^+ and D_s^+ lifetimes, themselves of some interest, and on $y_{\rm CP}$, based on the lifetime difference of $D^0 \to K^- K^+$ and $K^-\pi^+$.

*Speaker.

†I would like to thank Jun-ichi Tanaka for his help in preparing this talk, and the Japan Society for the Promotion of Science for financial assistance.

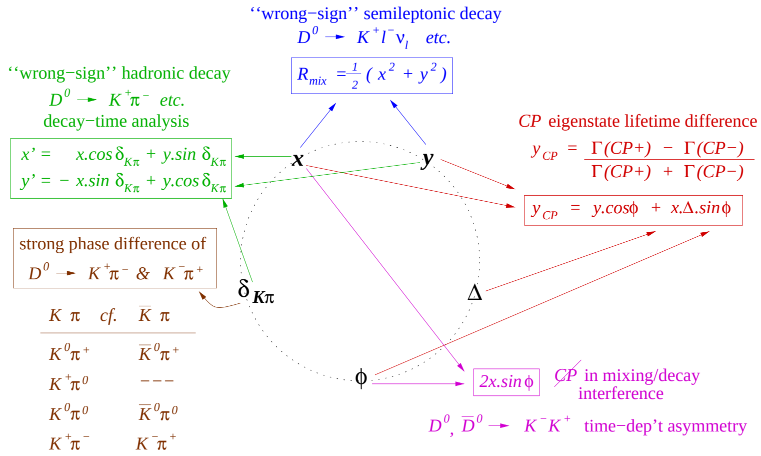

Figure 2: Quantities observed by various D-mixing experiments, and their relation to the parameters describing the mixing rate (x and y), CP-violating effects (Δ and ϕ), and the strong phase difference $\delta_{K\pi}$. Preliminary $D^0 \to K^0_L\pi^0$ results from Belle [7] promise new information on $\delta_{K\pi}$.

2. The Belle experiment

Belle is a general-purpose detector (figure 3) operating at the KEKB asymmetric energy e^+e^- collider. A 3-layer silicon vertex detector (SVD), 50-layer drift chamber (CDC), CsI(Tl) electromagnetic calorimeter (ECL) and particle-ID devices (time-of-flight [TOF] and aerogel Čerenkov counters [ACC]), are located within a 1.5 T solenoid; the flux return (KLM) is instrumented with RPCs to identify K^0_L and $\mu^\pm$.

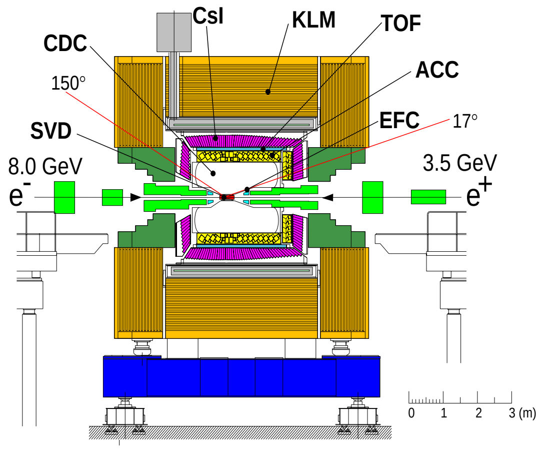

Figure 3: The Belle detector [8].

The analyses presented here rely on the good tracking ($\sigma_{p_T}/p_T = (0.19 p_T \oplus 0.3)\%$), impact parameter resolution ($\mathcal{O}(50\,\mu m)$) and particle-ID of Belle. Cuts on a likelihood ratio, combining dE/dx (CDC), TOF and ACC information, identify $K^\pm$ with $\epsilon \approx 85\%$ up to 3.5 GeV/c, with a $\pi^\pm$ fake-rate of $\approx 10\%$. Kaon (and pion) ID allows low-background D-meson reconstruction using inclusive samples, taking advantage of the large available dataset: 11.1 fb^{-1} (lifetimes) and 23.4 fb^{-1} (y_{CP}), collected near the $\Upsilon(4S)$ resonance.

	D^0		D^+		D^+_s	
	$K^-\pi^+$	K^-K^+	$K^-\pi^+\pi^+$	$\phi\pi^+$	$\phi\pi^+$	$\overline{K}^{*0}K^+$
11.1 fb^{-1}	90925 ± 352	7447 ± 134	6960 ± 100	1135 ± 39	3752 ± 57	2205 ± 68
23.4 fb^{-1}	214220 ± 558	18297 ± 189	–	–	–	–

Table 1: Fitted D-meson yields from 11.1 fb^{-1} and 23.4 fb^{-1} of Belle data.

3. Charm meson reconstruction

We reconstruct the decays $D^0 \to K^-\pi^+$ and K^-K^+, $D^+ \to K^-\pi^+\pi^+$ and $\phi\pi^+$, $D_s^+ \to \phi\pi^+$ and $\overline{K}^{*0}K^+$; charge-conjugate modes are included. We use CDC tracks with associated SVD hits, and track fits satisying χ^2/n.d.f < 5; particle-ID cuts are applied as noted above. D*-tagging is required only for $D^+ \to K^-\pi^+\pi^+$. The vector mesons ϕ, $\overline{K}^{*0}$ are recovered using $\phi \to K^-K^+$ and $\overline{K}^{*0} \to K^-\pi^+$, with an helicity angle cut $|\cos\theta_H| > 0.4$ applied.

We require $p_D > 2.5\,\mathrm{GeV}/c$ to eliminate B-daughters and suppress the combinatoric background. Decay angle cuts (*e.g.* $\cos\theta_D > -0.85$ for $D^0 \to K^-\pi^+$) are imposed to suppress random pions. Tracks are fit to a common vertex, and a cut χ^2/n.d.f < 3 is applied, rejecting poorly-measured candidates. The fitted momentum $\vec{p}_D$ is used to extrapolate the D to the interaction region and obtain the flight length.

The resulting D-meson samples are remarkably clean: examples are shown in figures 4 through 7, and the yields are listed in table 1.

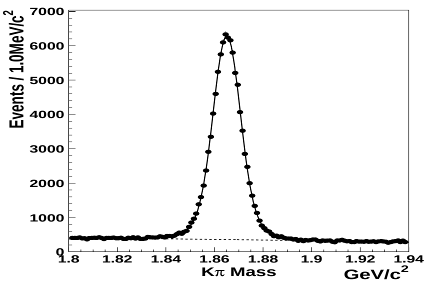

Figure 4: $D^0 \to K^-\pi^+$.

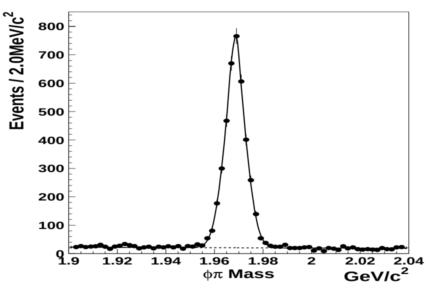

Figure 5: $D_s \to \phi\pi^+$.

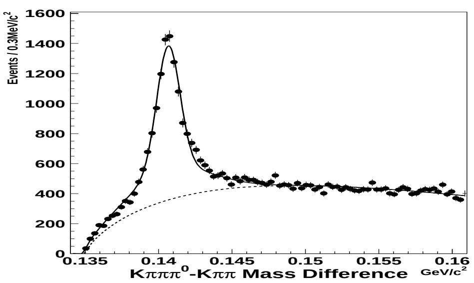

Figure 6: Mass-difference $M(K\pi\pi\pi^0) - M(K\pi\pi)$ for $D^{*+} \to D^+\pi^0$.

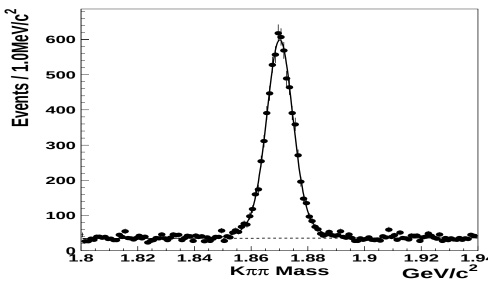

Figure 7: Mass distribution $M(K\pi\pi)$ for $D^+ \to K^-\pi^+\pi^+$ after D* cuts.

4. Charm lifetime measurement

To exploit the event-by-event errors σ_t^i on the proper times t^i of D-decays, we measure the D-lifetime τ_{SIG} using an unbinned maximum likelihood fit, with a likelihood function

$$\mathcal{L}(\tau_{SIG}, S, S_{tail}, f_{tail}, \tau_{BG}, f_{\tau_{BG}}, S_{BG}, S_{tail}^{BG}, f_{tail}^{BG}) =$$
$$\prod_i \Bigg[f_{SIG}^i \int_0^\infty dt' \frac{1}{\tau_{SIG}} e^{\frac{-t'}{\tau_{SIG}}} R(t^i - t'; \sigma_t^i, S, S_{tail}, f_{tail})$$
$$+(1 - f_{SIG}^i) \int_0^\infty dt' \{ f_{\tau_{BG}} \frac{1}{\tau_{BG}} e^{\frac{-t'}{\tau_{BG}}} + (1 - f_{\tau_{BG}})\delta(t') \} R(t^i - t'; \sigma_t^i, S_{BG}, S_{tail}^{BG}, f_{tail}^{BG}) \Bigg],$$

where f^i_{SIG} is the signal probability, based on the D-mass distribution. A double-Gaussian signal resolution function is used, with tail fraction f_{tail}, and scaling factors S and S_{tail} for σ^i_t. The background is modelled as a fraction $f_{\tau_{BG}}$ with lifetime (*e.g.* charm daughters) and a fraction $(1 - f_{\tau_{BG}})$ without, with a common "resolution". The fit includes D-candidates within $\pm 40\,\mathrm{MeV}/c^2$ ($\approx 6\sigma$) of the mean D-mass. For each of D^+ and D^+_s a single fit is performed, using a combined likelihood (for D^+) $\mathcal{L} = \mathcal{L}_{\mathrm{K}\pi\pi} \cdot \mathcal{L}_{\phi\pi}$, with a common lifetime τ_{SIG}. The D^+ fit result is shown, together with $\mathrm{D}^+ \to \mathrm{K}^-\pi^+\pi^+$ data, in figures 8 and 9.

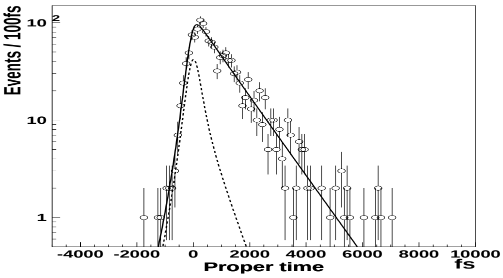

Figure 8: D^+ fit: the $\mathrm{D}^+ \to \mathrm{K}^-\pi^+\pi^+$ signal region $|\Delta M| \leq 3\sigma_M$. The dashed line shows the background component.

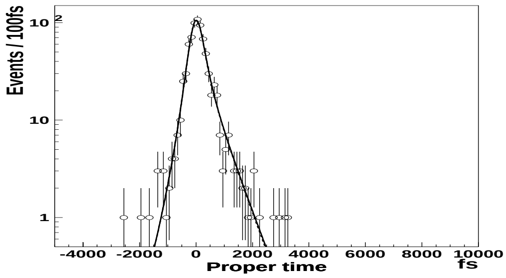

Figure 9: D^+ fit: the $\mathrm{D}^+ \to \mathrm{K}^-\pi^+\pi^+$ background-dominated region $3\sigma_M < |\Delta M| \leq 6\sigma_M$.

The lifetimes of the three species are listed in table 2, including corrections for biasses, estimated from the Monte Carlo simulation. Systematic error contributions are shown in table 3: uncertainties in the effect of the vertexing cuts, and the bias corrections, are dominant. Note that the resolution on D-lifetime ratios from this experiment alone has reached the percent level: $\tau(\mathrm{D}^+)/\tau(\mathrm{D}^0) = 2.50 \pm 0.03^{+0.01}_{-0.02}$, and $\tau(\mathrm{D}^+_s)/\tau(\mathrm{D}^0) = 1.17 \pm 0.02 \pm 0.01$.

$\tau(\mathrm{D}^0)$ fs	$\tau(\mathrm{D}^+)$ fs	$\tau(\mathrm{D}_s)$ fs
$414.6 \pm 1.7^{+1.9}_{-1.8}$	$1037 \pm 12^{+5}_{-6}$	$485.4^{+7.9+2.9}_{-7.7-4.2}$

Table 2: Lifetime fits: summary of results.

5. The y_{CP} analysis

We measure y_{CP} using the larger (23.4 fb^{-1}) data sample, fitting $\mathrm{D}^0 \to \mathrm{K}^-\pi^+$ and $\mathrm{K}^-\mathrm{K}^+$ with a combined likelihood function $\mathcal{L} = \mathcal{L}_{\mathrm{K}^-\pi^+} \cdot \mathcal{L}_{\mathrm{K}^-\mathrm{K}^+}$, where we set $\tau_{\mathrm{K}^-\mathrm{K}^+} = \tau_{\mathrm{K}^-\pi^+}/(1 + y_{\mathrm{CP}})$. The fit result is compared to the $\mathrm{D}^0 \to \mathrm{K}^-\mathrm{K}^+$ data in the $|\Delta M| < 3\sigma_M$ region in figure 10. We find $y_{\mathrm{CP}} = 0.5 \pm 1.0^{+0.8}_{-0.9}$, corresponding to a 95% confidence interval $-2.1\% < y_{\mathrm{CP}} < 3.1\%$. The result includes a correction for fit bias, which dominates the systematic error (table 3): many other sources of error, which are similar for the two decay modes, cancel.

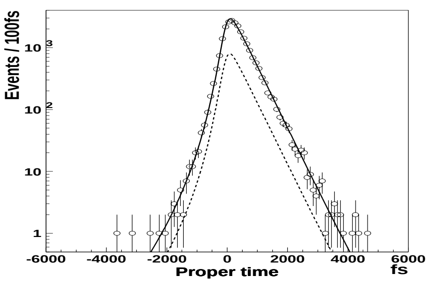

Figure 10: y_{CP} fit: the $\mathrm{D}^0 \to \mathrm{K}^-\mathrm{K}^+$ signal region.

Source	error (fs)			error (fraction of %)
	$D^0 \to K^-\pi^+$	D^+	D_s^+	y_{CP}
IP size, position	± 0.2	$^{+0.4}_{-0.3}$	$^{+0.1}_{-0.8}$	$^{+0.1}_{-0.3}$
vertexing cuts	$^{+0.5}_{-0.4}$	$^{+0.0}_{-3.2}$	$^{+0.0}_{-2.9}$	$^{+0.11}_{-0.43}$
decay length bias	± 1.1	$^{+1.8}_{-1.7}$	± 1.8	± 0.01
PDG D mass	± 0.1	± 0.3	± 0.1	± 0.05
mass-time correlation	$^{+0.02}_{-0.03}$	$^{+0.0}_{-0.2}$	$^{+0.05}_{-0.04}$	$^{+0.04}_{-0.02}$
error on f_{SIG}	$^{+0.1}_{-0.2}$	$^{+1.8}_{-2.0}$	± 0.5	± 0.06
D mass sideband	$^{+0.4}_{-0.3}$	$^{+0.0}_{-0.6}$	$^{+0.02}_{-0.20}$	$^{+0.21}_{-0.09}$
fit bias	± 1.1	± 4.3	± 2.1	± 0.71
TOTAL	$^{+1.9}_{-1.8}$	$^{+5.0}_{-6.0}$	$^{+2.9}_{-4.2}$	$^{+0.80}_{-0.88}$

Table 3: Lifetime and y_{CP} fits: systematic errors.

6. Conclusion

Belle preliminary results on D-lifetimes and y_{CP} are competitive with the current world averages (table 4). Our y_{CP} measurement is consistent with zero. These results will be finalized and published soon, when the ongoing study of systematic effects is complete.

Experiment	$\tau(D^0)$ fs	$\tau(D^+)$ fs	$\tau(D_s)$ fs	y_{CP} (%)
E687	$413 \pm 4 \pm 4$	$1048 \pm 15 \pm 11$	$475 \pm 20 \pm 7$	–
E791	$413 \pm 3 \pm 4$	–	$518 \pm 14 \pm 7$	$0.8 \pm 2.9 \pm 1.0$
CLEO	$408.5 \pm 4.1^{+3.5}_{-3.4}$	$1034 \pm 22^{+10}_{-13}$	$486 \pm 15 \pm 5$	$-1.1 \pm 2.5 \pm 1.4$
PDG	412.6 ± 2.8	1051 ± 13	496^{+10}_{-9}	–
FOCUS	409.2 ± 1.3	–	506 ± 8	$3.42 \pm 1.39 \pm 0.74$
Belle	$414.6 \pm 1.7^{+1.9}_{-1.8}$	$1037 \pm 12^{+5}_{-6}$	$485.4^{+7.9+2.9}_{-7.7-4.2}$	$0.5 \pm 1.0^{+0.8}_{-0.9}$

Table 4: Current D-lifetime and y_{CP} measurements: Belle results are preliminary.

References

[1] I. Bigi and N. Uraltsev, *Nucl. Phys.* **B 592** (2001) 92. `hep-ph/0005089`.

[2] E. Aitala *et. al.*, *Phys. Rev. Lett.* **77** (1996) 2384. `hep-ex/9606016`.

[3] R. Godang *et. al.*, *Phys. Rev. Lett.* **84** (2000) 5038. `hep-ex/0001060`.

[4] E. Aitala *et. al.*, *Phys. Rev. Lett.* **83** (1999) 32. `hep-ex/9903012`.

[5] J. Link *et. al.*, *Phys. Lett.* **B 485** (2000) 62. `hep-ex/0004034`

[6] D. Cronin-Hennessy *et. al.*, `hep-ex/0102006`.

[7] S. Semenov, *Study of charmed baryon decays and $D^0 \to K^0\pi^0$ decay at Belle*, *J. High Energy Phys.* **PRHEP-hep2001** (2001) 107; K. Abe *et. al.*, `hep-ex/0107078`.

[8] K. Abe *et. al.*, *The Belle detector*, KEK Progress Report 2000–04. To be published in Nucl. Instr. and Meth. in Phys. Res. A.